

Rethinking Scientific Modeling: Toward Physically Consistent and Simulation-Executable Programmatic Generation

Yongqing Jiang

Sichuan University

Chengdu, China

yongqingjiang@stu.scu.edu.cn

Zhenghong Lin

Nanyang Technological University

Singapore, Singapore

hongzhenglin970323@gmail.com

Jianze Wang

Sichuan University

Chengdu, China

jzwang@scu.edu.cn

Jiayuan Wang

Fuzhou University

Fuzhou, China

241027217@fzu.edu.cn

Zhiqi Shen

Nanyang Technological University

Singapore, Singapore

zqshen@ntu.edu.sg

Yijian Yang

Sichuan University

Chengdu, China

yijianyang@alu.scu.edu.cn

Kaoshan Dai^{*}

Sichuan University

Chengdu, China

kdai@scu.edu.cn

Haoran Luo^{*}

Nanyang Technological University

Singapore, Singapore

haoran.luo@ieee.org

Abstract

Structural modeling is a fundamental component of computational engineering science, in which even minor physical inconsistencies or specification violations may invalidate downstream simulations. The potential of large language models (LLMs) for automatic generation of modeling code has been demonstrated. However, non-executable or physically inconsistent outputs remain prevalent under stringent engineering constraints. A framework for physics-consistent automatic building modeling is therefore proposed, integrating domain knowledge construction, constraint-oriented model alignment, and verification-driven evaluation. CivilInstruct is introduced as a domain-specific dataset that formalizes structural engineering knowledge and constraint reasoning to enable simulation-ready model generation. A two-stage fine-tuning strategy is further employed to enforce constraint satisfaction and application programming interface compliance, substantially reducing hallucinated and non-conforming outputs. MBEval is presented as a verification-driven benchmark that evaluates executability and structural dynamics consistency through closed-loop validation. Experimental results show consistent improvements over baselines across rigorous verification metrics. Our code is available at <https://github.com/Jovanqing/AutoBM>.

CCS Concepts

• Computing methodologies → Artificial intelligence.

Keywords

Physics-constrained Learning, Automatic Building Modeling, Structural Engineering, Scientific Modeling

1 Introduction

Accurate numerical modeling is a cornerstone of computational structural science. Recent advances in large language models (LLMs) [2, 29, 38, 40] introduce a new paradigm for scientific modeling.

^{*}Corresponding authors

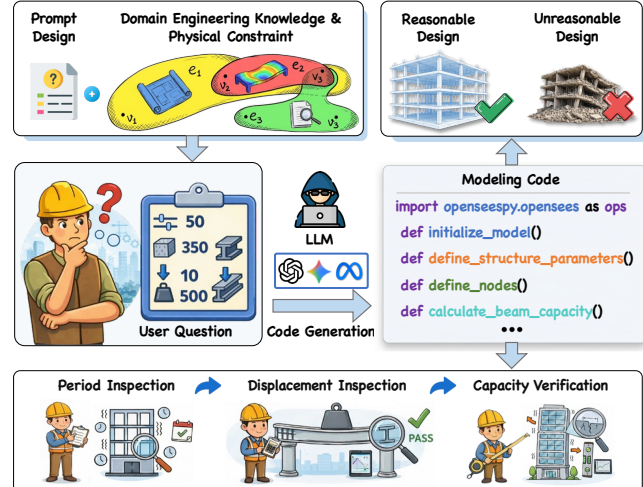


Figure 1: Task formulation of LLM-driven automatic building modeling from natural language descriptions

As shown in Figure 1, LLMs can interpret natural-language specifications and generate corresponding structural modeling code [15, 18, 36], enabling automated construction of simulation-ready models. Within this emerging paradigm, structural modeling stands out as a compelling domain due to its complexity, rule constraints, and reliance on expert knowledge. OpenSeesPy is a cornerstone platform for seismic and structural analysis [4, 35, 44, 53] due to its strong capability in simulating complex structural systems (Figure 2(a)). When integrated with OpenSeesPy and multi-source data (Fig. 2(b)), LLMs enable automatic building modeling (AutoBM) across multiple building types by directly generating modeling code. Relative to rule-based template methods (Fig. 2(c)), LLM-driven modeling offers superior scalability, positioning it as a promising computational interface for engineering simulation.

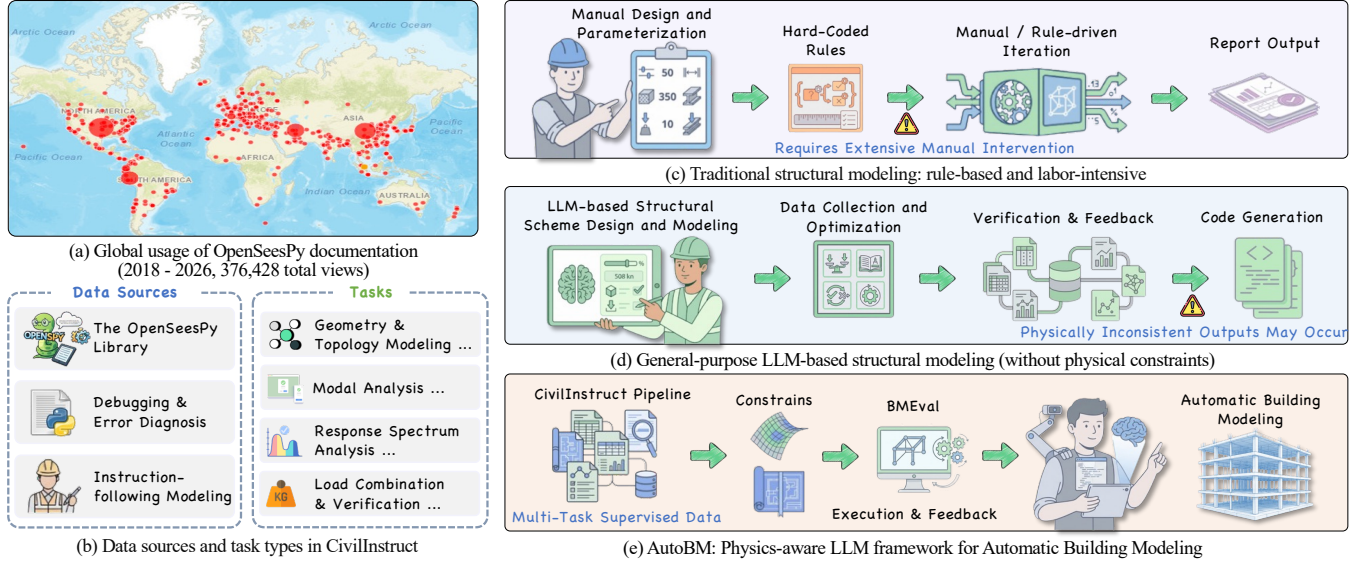


Figure 2: Overview of this study, illustrating the integration of large language models with structural engineering knowledge for Automatic Building Modeling (AutoBM), including task motivation, data foundations, and the framework

Despite this promise, existing LLM-based approaches to structural modeling remain fundamentally limited. Automated approaches based on LLMs are increasingly applied to modeling research (e.g., structural verification [27], 2D frame modeling [12], integration with the computational engine [26] of OpenSeesPy). These LLM-driven modeling approaches [5, 6, 8] have been shown to improve the efficiency of building modeling. However, prior work largely overlooks task-specific fine-tuning for structural engineering, despite the domain's strict requirements on engineering compliance beyond syntactic correctness. As shown in Figure 2(d), without domain-specific knowledge integration, ensuring the model's physical correctness is difficult for general-purpose LLMs.

This raises a key question: *"How can LLMs be systematically constrained to enable structurally and physically valid programmatic generation for building modeling?"* To address this question, we propose a physics-aware LLM framework for AutoBM, as shown in Figure 2(e). The main contributions of this work can be summarized as follows:

- **Novel AutoBM Task:** We formalize Automatic Building Modeling (AutoBM) as a research task with clearly defined problem boundaries. The task specifies user-driven modeling requirements by defining task inputs (building function, plan dimensions) and task outputs (engineering-compliant, high-precision structural modeling code).
- **BMBench Dataset:** We propose BMBench, a comprehensive AutoBM benchmark integrating large-scale instruction data and multidimensional evaluation metrics across 10,912 samples and 128 cases.
- **RLA-SPC:** We propose a reinforcement learning alignment strategy under structural physical constraints, and experimental results show that RLA-SPC improves LLM compliance with engineering physical constraints.

2 Related Work

Large Language Models. General-purpose LLMs [1, 10, 45] exhibit limited generalization in specialized domains, prompting domain adaptation efforts and the development of domain-specific benchmarks across medicine [37], finance [41], and biology [30]. Within the civil engineering domain, applied research on LLMs exhibits a trend toward multifaceted breakthroughs. For example, Kim et al. [22] and Pandey et al. [32] demonstrated the feasibility of using LLMs to generate high-fidelity simulation codes for fluid-structure interaction and computational fluid dynamics (CFD), respectively. Qin et al. [33] developed an intelligent shear wall design framework that achieved substantial gains in design efficiency while satisfying mechanical constraints. Jiang et al. [20, 21] and Jeoung et al. [19] applied visual-language modeling techniques to automate visual analytics tasks, including post-earthquake damage assessment and construction site monitoring.

Automatic Structural Modeling and Reasoning. Early computational approaches for design-analysis mapping mainly relied on rigid scripting interfaces [17, 28, 49] or parametric template-based generation methods [7, 14, 31, 52]. With the emergence of LLMs, existing studies have explored domain adaptation through model fine-tuning [43] and the integration of structured domain knowledge (e.g., knowledge graphs [24, 46], material mechanism discovery [16], energy system optimization [13]). More recent research has further advanced toward system-level reasoning by adopting multi-agent collaboration mechanisms [9, 23, 47], while the incorporation of chain-of-thought reasoning and literate programming paradigms has enabled LLMs to orchestrate end-to-end simulation pipelines [50], motivating the development of domain-specific benchmarks for systematic evaluation of LLM-driven engineering automation [3, 11, 25, 39].

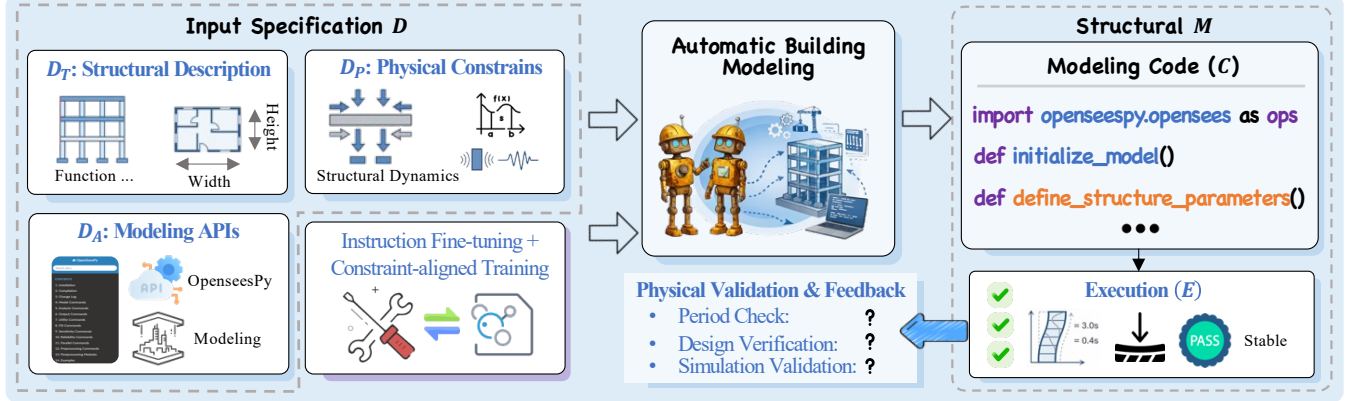


Figure 3: The definition and overview of the AutoBM task.

3 Task: AutoBM

The AutoBM task is formally defined as the process of generating executable, physically consistent structural modeling code from structured engineering specifications using LLMs. As shown in Figure 3, the fundamental objective of AutoBM is to bridge the gap between natural language intent and rigorous structural engineering requirements while strictly adhering to physical constraints. Formally, a building modeling specification is defined as $\mathcal{S} = (D_T, D_P, D_A)$. In this formulation, the textual description of the structural modeling task, including building geometry, building function, and seismic intensity, is denoted by D_T . The set of physical and engineering constraints (e.g., structural mechanics principles, design verification requirements) is represented by D_P . Furthermore, the target modeling APIs and the computational environment (e.g., OpenSeesPy functions, modeling workflows) are specified by D_A . Given this specification, the modeling target is characterized as a structural model implementation $\mathcal{M} = (C, E)$, where C represents the generated modeling code and E represents the execution outcomes. These outcomes encompass successful compilation, runtime stability, and physically valid responses (e.g., modal periods, internal forces).

The AutoBM task is characterized as the generation of an optimal structural model \hat{M} , conditioned upon the input specification D . This optimization objective is formulated as:

$$\hat{M} = \arg \max_M \Pr(M | D) \quad (1)$$

In contrast to general-purpose code-generation paradigms, the AutoBM task requires the generated code to satisfy constraints on both syntactic correctness and physical feasibility. Consequently, the optimization objective is characterized as multi-dimensional. A composite objective function $\vec{F}(M)$ is formulated as follows:

$$\max \vec{F}(M) = \alpha_1 S_{\text{Exec}}(M | D_A) + \alpha_2 S_{\text{Phys}}(M | D_P) + \alpha_3 S_{\text{Spec}}(M | D_T) \quad (2)$$

Here, $S_{\text{Exec}}(M | D_A)$ evaluates executability and API compliance, while $S_{\text{Phys}}(M | D_P)$ measures physical consistency and structural validity under mechanics principles and engineering constraints. Semantic alignment with modeling requirements is assessed by

$S_{\text{Spec}}(M | D_T)$. The trade-offs among these objectives are regulated by non-negative weights α_i , balancing code flexibility and physical correctness. The objective of AutoBM is therefore to generate executable, engineering-valid structural models, thereby forming a closed-loop paradigm for LLM-based building modeling.

4 BenchMark: BMBench

This section introduces the modeling of building benchmark (BMBench), a novel benchmark designed for the training and evaluation of AutoBM task. The construction process, evaluation protocol, and the metrics derived from this protocol are described in detail.

4.1 CivilInstruct Dataset Construction

The construction of the CivilInstruct dataset follows a four-stage pipeline, as shown in Figure 4. First, OpenSeesPy documentation was combined with LLM-based synthesis to generate 3,800 API-learning samples and 3,100 expert-level instruction-code instances covering building functions and seismic conditions. Subsequently, 3,500 Bug-CoT samples were derived from execution error logs, and 512 high-quality code instances were filtered and annotated with structural periods obtained via finite element analysis, providing physically grounded supervisory signals. Further implementation details for each stage are provided in Appendix A.1.

4.2 BMEval: Benchmark Design

To ensure the quality, relevance, and effectiveness of the AutoBM task, BMEval was constructed through a three-stage process. First, building samples were randomly generated to cover a diverse set of attributes (e.g., building function, floor height, plan dimensions) within a reasonable structural parameter space. Then, an expert-driven mechanism was adopted to optimize and validate all design solutions in strict accordance with seismic design codes, ensuring their structural feasibility and executability. Subsequently, empirical formulas were used to compute the fundamental period of each structure as ground-truth reference values. In total, 128 labeled evaluation samples were obtained, each containing complete building information and its corresponding structural period.

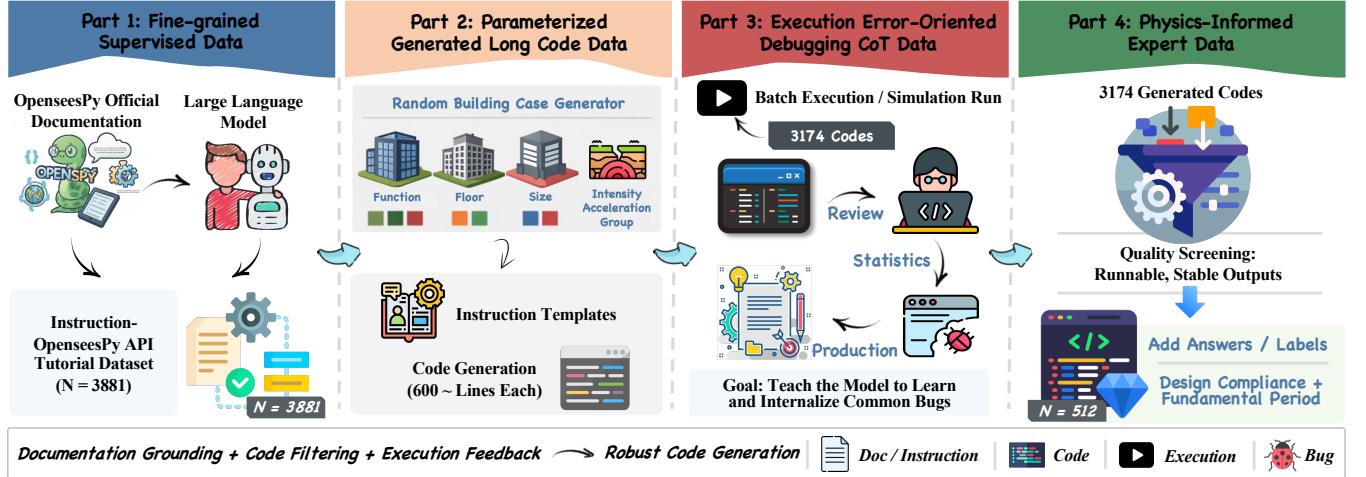


Figure 4: Overview of the CivilInstruct construction procedure.

To evaluate LLM performance on the AutoBM task, we adopt a multidimensional evaluation protocol covering program executability, computational accuracy, and engineering compliance. For each test sample, the model independently generates n candidate programs, which are executed sequentially in a restricted sandbox. A program is deemed successful if it terminates normally within the prescribed time limit.

Following the standard evaluation paradigm of mainstream code-generation benchmarks (e.g., HumanEval [34], MBPP [48]), we employ the unbiased $Pass@k$ estimator to measure the probability that at least one valid solution is obtained:

$$pass@k = \begin{cases} 1, & n \leq k, \\ 1 - \frac{\binom{n-c}{k}}{\binom{n}{k}}, & \text{otherwise.} \end{cases} \quad (3)$$

Building upon $Pass@k$, we further define three task-specific metrics: $Pass@k_{\text{period}}$, $Pass@k_{\text{compliance}}$, and $Pass@k_{\text{strict}}$, corresponding to structural cycle consistency, engineering compliance, and their joint assessment. Formal definitions of these metrics are provided in Appendix A.2. See Appendix B for the prompt used to construct the BMBenchmark.

5 Methodology: Two-Stage Reinforcement Learning Alignment Under Structural Physical Constraints

We formulate AutoBM as a conditional program synthesis problem. Given an engineering instruction x (e.g., building function, plan dimensions), a language model parameterized by θ defines a conditional policy $\pi_\theta(\cdot | x)$ over OpenSeesPy code sequences $y = (y_1, \dots, y_T)$. Our goal is to learn π_θ that produces code that is (i) domain-compliant, (ii) logically complete, and (iii) physically valid under structural mechanics constraints. To this end, we propose **RLA-SPC**, a two-stage reinforcement learning framework for aligned policy optimization. As shown in Algorithm 1, the policy

is first initialized via supervised fine-tuning to ensure basic executability, and subsequently optimized using SPC-GRPO to enforce structured and physics-aware constraints.

5.1 Stage I: Domain Instruction Fine-Tuning

Let $\mathcal{D} = \{(x^{(n)}, y^{(n)})\}_{n=1}^N$ denote the instruction dataset (CivilInstruct), where x is an AutoBM instruction and y is a reference OpenSeesPy implementation. We fine-tune a pretrained model by maximizing the conditional likelihood of the reference code:

$$\mathcal{L}_{\text{SFT}}(\theta) = -\mathbb{E}_{(x, y) \sim \mathcal{D}} \left[\sum_{t=1}^{|y|} \log \pi_\theta(y_t | x, y_{<t}) \right]. \quad (4)$$

The policy is denoted as π_{ref} (the *reference policy*), which captures domain syntax, OpenSeesPy API usage patterns, and engineering priors. However, SFT alone does not guarantee physical validity because it does not explicitly optimize for physics-based criteria.

5.2 Stage II: Structural Physics-Constrained Reinforcement Learning Alignment

To explicitly enforce physical consistency, we further align the model using a structural physics-constrained variant of group-relative policy optimization (SPC-GRPO). SPC-GRPO follows the group-relative optimization paradigm, while incorporating domain-specific physical constraints via a multi-granularity hybrid reward and a reference-policy KL regularization. For each query q (we use $q \equiv x$), we sample a group of G candidate outputs $\{o_i\}_{i=1}^G \sim \pi_{\theta_{\text{old}}}(\cdot | q)$.

In SPC-GRPO, instead of learning a separate value function, the advantage is estimated using an in-group baseline:

$$\bar{R} = \frac{1}{G} \sum_{i=1}^G R(o_i), \quad s_R = \sqrt{\frac{1}{G} \sum_{i=1}^G (R(o_i) - \bar{R})^2 + \varepsilon}, \quad (5)$$

$$\hat{A}_i = \frac{R(o_i) - \bar{R}}{s_R}. \quad (6)$$

The policy is updated by maximizing the following objective function, which promotes candidate solutions with higher relative physical quality while regularizing the policy update through a reference-policy KL constraint:

$$\mathcal{J}(\theta) = \mathbb{E} \left[\frac{1}{G} \sum_{i=1}^G \frac{\pi_\theta(o_i|q)}{\pi_{\theta_{\text{old}}}(o_i|q)} \hat{A}_i - \beta \mathbb{D}_{\text{KL}}(\pi_\theta(\cdot|q) \parallel \pi_{\text{ref}}(\cdot|q)) \right], \quad (7)$$

where π_{ref} is the frozen SFT policy. This formulation encourages outputs with higher relative physical quality while preventing excessive deviation from the reference distribution.

5.3 Multi-Granularity Hybrid Reward

Central to our alignment strategy is the design of the reward function. Specifically, for a generated solution o , we formulate a Multi-Granularity Hybrid Reward (MGHR) as follows:

$$R(o) = w_{\text{fmt}} r_{\text{fmt}}(o) + w_{\text{ast}} r_{\text{ast}}(o) + w_{\text{exec}} r_{\text{exec}}(o), \quad (8)$$

where w_{fmt} , w_{ast} , and w_{exec} denote the weighting coefficients assigned to the respective components of the reward function. In this study, these weights are set to 0.05, 0.25, and 0.70, respectively. This distribution reflects the hierarchy of core engineering principles, where physical correctness constitutes the ultimate criterion, logical correctness serves as a necessary precondition, and formatting constraints fulfill a supplementary regulatory role.

5.3.1 Format Compliance Reward. The reward r_{fmt} is designed to enforce a strict output structure, ensuring compliance with Markdown code blocks and reasoning tags. It is formally defined as:

$$r_{\text{fmt}}(o) = \mathbb{I}[\text{FormatOK}(o)], \quad (9)$$

where $\text{FormatOK}(\cdot)$ denotes a deterministic parser implemented via regular expressions.

5.3.2 Logical Completeness via Hierarchical AST. Before execution, we assess whether the generated code is logically complete. Let $\text{API}(o)$ be the set of APIs extracted from the AST of o . We construct three-tiered API sets: \mathcal{T}_1 for topology APIs, \mathcal{T}_2 for boundary and load APIs, and \mathcal{T}_3 for analysis and solver APIs.

Tier-wise coverage is defined as:

$$c_k(o) = \frac{|\text{API}(o) \cap \mathcal{T}_k|}{|\mathcal{T}_k|}. \quad (10)$$

We further penalize undefined variables detected by static analysis. The logical reward is:

$$\tilde{r}_{\text{ast}}(o) = \sum_{k=1}^3 \alpha_k c_k(o) - \lambda N_{\text{undef}}(o), \quad r_{\text{ast}}(o) = \text{clip}(\tilde{r}_{\text{ast}}, 0, 1). \quad (11)$$

5.3.3 Sandbox-Based Physical Consistency. Finally, we evaluate physical correctness by executing the code in an OpenSees sandbox:

$$r_{\text{exec}} = \begin{cases} \eta_{\text{env}}, & \text{if env. error or timeout} \\ R_{\text{prog}}(l_{\text{err}}, L_{\text{tot}}), & \text{if runtime logic error} \\ R_{\text{phy}}(\epsilon), & \text{if success with physical metrics} \end{cases} \quad (12)$$

Algorithm 1: RLA-SPC

Input: Instruction dataset $\mathcal{D} = \{(x^{(n)}, y^{(n)})\}_{n=1}^N$; group size G ; KL weight β ; MGHR weights $(w_{\text{fmt}}, w_{\text{ast}}, w_{\text{exec}})$.

Output: Aligned policy $\pi_\theta(\cdot| x)$.

Stage I (SFT): Initialize θ from a pretrained model;

while not converged **do**

 Sample minibatch $\mathcal{B} \subset \mathcal{D}$;

 Update $\theta \leftarrow \theta - \eta \nabla_\theta \mathcal{L}_{\text{SFT}}(\theta; \mathcal{B})$ using Eq. (4);

 Freeze $\pi_{\text{ref}} \leftarrow \pi_\theta$;

Stage II (SPC-GRPO): **while** not converged **do**

 Sample a batch of queries $Q = \{q\}$ where $q \equiv x$;

 Set $\theta_{\text{old}} \leftarrow \theta$;

foreach $q \in Q$ **do**

 Sample G candidates $\{o_i\}_{i=1}^G \sim \pi_{\theta_{\text{old}}}(\cdot|q)$;

foreach o_i **do**

 Compute format reward $r_{\text{fmt}}(o_i)$ via Eq. (9);

 Compute tier-wise coverage $c_k(o_i)$ via Eq. (10) and AST reward $r_{\text{ast}}(o_i)$ via Eq. (11);

 Execute o_i in sandbox and compute $r_{\text{exec}}(o_i)$ via Eqs. (12)–(15) (including progress reward Eq. (13) and period error Eq. (14));

 Aggregate $R(o_i)$ via Eq. (8);

 Compute \tilde{R}, s_R via Eq. (5) and advantages \hat{A}_i via Eq. (6);

 Update $\theta \leftarrow \arg \max_\theta \mathcal{J}(\theta)$ using Eq. (7);

For runtime failures, we use execution progress:

$$R_{\text{prog}} = \alpha_{\text{base}} + \beta_{\text{step}} \frac{l_{\text{err}}}{L_{\text{tot}}}. \quad (13)$$

where l_{err} represents the specific line number of the reported error as captured by the interpreter traceback, and L_{tot} denotes the total number of code lines. The parameter α_{base} signifies the base attempt reward, which is utilized to incentivize the successful initiation of the execution stage. Furthermore, β_{step} is defined as the progress scaling factor, employed to modulate the contribution of code completion to the overall score.

For successful executions, physical consistency is evaluated using the relative error of the structural fundamental period.

$$\epsilon = \frac{|T_{\text{pred}} - T_{\text{gt}}|}{T_{\text{gt}}}, \quad (14)$$

$$R_{\text{phy}}(\epsilon) = \begin{cases} 1.00, & \epsilon \leq 0.10, \\ 0.90, & 0.10 < \epsilon \leq 0.20, \\ 0.80, & 0.20 < \epsilon \leq 0.40, \\ 0.70, & \text{otherwise.} \end{cases} \quad (15)$$

This hierarchical reward design explicitly reflects the tolerance-based decision paradigm commonly adopted in structural engineering practice, where approximate physical consistency is often acceptable within specified error bounds, while larger deviations are progressively penalized.

Table 1: Main results on BMEval.

Model Name	Executability		Engineering-Level Output Evaluation			Overall Average	
	Pass@1	Pass@5	Pass@5 _{period}	Pass@5 _{compliance}	Pass@5 _{strict}		
DeepSeek-Coder-6.7B	8.59	17.97	1.56	0.78	0.00	0.78	4.95
Qwen2.5-Coder-7B-Instruct	10.94	19.53	1.56	3.91	0.78	2.08	6.47
CodeLlama-7B-Instruct	7.03	17.19	2.34	4.69	0.00	2.34	5.60
Opencoder-8B-Instruct	9.25	18.75	0.78	2.34	0.78	1.30	5.53
Seed-coder-8B^R	11.72	21.09	0.78	3.13	0.78	1.56	6.51
DeepSeek-V3.2^R	7.81	12.50	1.56	2.34	0.00	1.30	4.25
DeepSeek-R1^R	5.47	10.94	0.78	3.13	0.78	1.56	3.78
GLM-4.6	3.13	10.16	1.56	1.56	0.00	1.04	2.91
Qwen3-Coder-Plus	13.28	28.91	1.56	3.91	0.78	2.08	8.42
Qwen3-Coder-480B-A35B-Instruct	12.19	25.78	2.34	4.69	1.56	2.86	8.24
GPT-5^R	32.81	58.59	22.66	32.03	11.72	22.14	29.99
GPT-5-nano	13.28	34.38	4.69	13.06	1.56	6.44	12.24
Gemini-2.5-Flash	41.41	75.78	7.03	17.97	5.47	10.16	26.30
Gemini-3-pro-Preview^R	26.56	53.91	32.28	34.09	16.62	27.66	31.85
Grok-Code-Fast	18.62	43.84	12.84	18.57	9.16	13.52	19.43
Claude-Sonnet-4.5^R	51.38	79.34	20.41	49.13	18.84	29.46	41.43

Note: “R” denotes reasoning models. Boldface indicates the best result. “Average” is the mean of Pass@5_{period}, Pass@5_{compliance}, Pass@5_{strict}. “Overall Average” is the mean of Pass@1, Pass@5, Pass@5_{period}, Pass@5_{compliance}, Pass@5_{strict}, and “Average”.

Table 2: Performance comparison on AutoBM before and after applying RLA-SPC.

Model Name	Executability		Engineering-Level Output Evaluation			Overall Average	
	Pass@1	Pass@5	Pass@5 _{period}	Pass@5 _{compliance}	Pass@5 _{strict}		
CodeLlama-7B-Instruct	7.03	17.19	2.34	4.69	0.00	2.34	5.60
+ RLA-SPC	55.73	91.34	69.91	85.32	67.73	74.32	74.06
Qwen2.5-Coder-7B	10.94	19.53	1.56	3.91	0.78	2.08	6.47
+ RLA-SPC	61.27	94.31	73.84	87.65	71.82	77.77	77.78
Seed-Coder-8B-R^R	11.72	21.09	0.78	3.13	0.78	1.56	6.51
+ RLA-SPC	64.18	97.28	78.05	92.47	77.14	82.55	81.95

6 Experiments and Analysis

6.1 Experimental Setup

To evaluate LLM performance on the AutoBM task, a set of representative state-of-the-art open-source and commercial models was assessed using the BMEval benchmark, which consists of 128 automated modeling tasks designed to cover diverse structural configurations and seismic conditions. All models were evaluated under a unified protocol, and the main results are summarized in Table 1 and Figure 5(a).

6.2 Limitations of LLMs for the AutoBM Task

Although leading models such as Claude-Sonnet-4.5^R and GPT-5^R achieve high code execution rates, their joint evaluation scores remain low, indicating significant limitations in practical engineering applicability under realistic design constraints.

Grammatical and physical divide. Models exhibit a systematic mismatch between syntactic correctness and physical validity. For instance, Gemini-2.5-Flash attains a high Pass@5 score (75.78%) but an extremely low Pass@5_{strict} score (5.47%), suggesting that physical parameters are treated as statistical symbols rather than physically constrained quantities. Consequently, models frequently generate simulations that are syntactically valid but physically implausible under realistic design constraints.

Spatial-topological reasoning. Performance on the AutoBM task remains limited. Gemini-3-Pro-Preview achieves the highest structural prediction accuracy (Pass@5 = 32.28%), while other leading models perform moderately, and most open-source models score below 3%. These results indicate persistent difficulties in maintaining consistent geometric representations, with no clear scaling trend with model size.

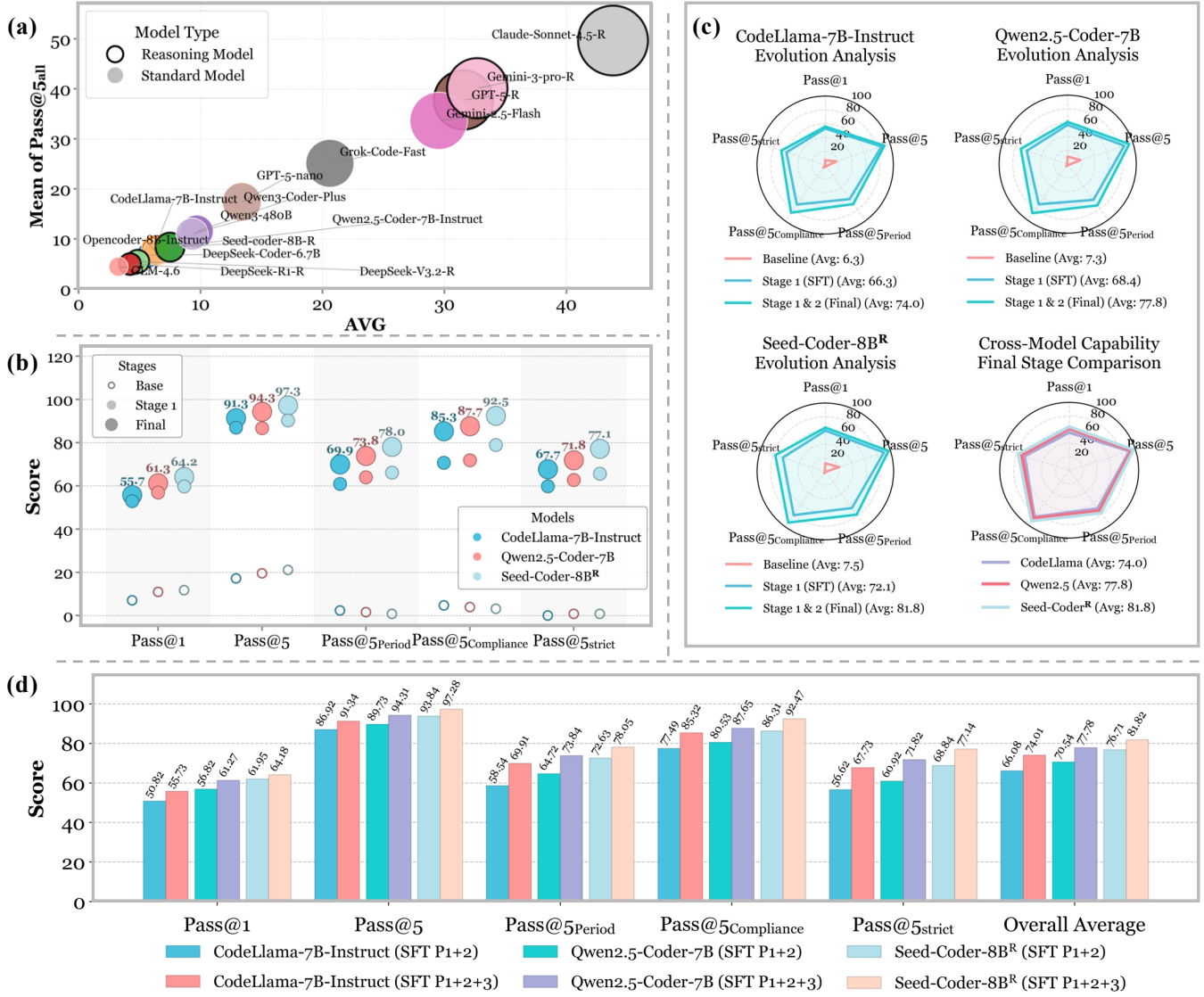


Figure 5: The results of the report generation tasks. (a) LLM performance on the BMEval benchmark. (b) & (c) Evolution of model performance across training stages. (d) Impact of data composition on baseline models

Engineering self-verification. Closed-loop reasoning remains weak across models. Although Claude-Sonnet-4.5^R achieves relatively better compliance ($\text{Pass}@5_{\text{compliance}} = 49.13\%$), most models fail to perform specification-driven verification, even under explicit constraint prompts. Overall, current LLMs lack reliable multi-step reasoning capabilities for engineering compliance.

To further investigate the training dynamics, Figures 5(b-d) and Table 2 illustrate the performance evolution and the impact of data composition. The analysis indicates that the second stage of training is critical for improving compliance-related metrics (see Figures 5(b) and 5(c)), and that data matching plays a pivotal role in determining training effectiveness (see Figure 5(d)). A comprehensive analysis of the training stages and the ablation studies presented in Figures 5(b-d) is provided in Appendix C.

6.3 Case Study: Failure Mode Analysis in AutoBM

To further investigate the limitations of AutoBM, a systematic code inspection of the LLM-generated code was conducted. As shown in Figure 6(a), the observed failure modes were primarily categorized into three types: executability, compliance, and period.

The overall error distribution was markedly skewed. Executability failures dominated (87.5%), whereas compliance and period failures accounted for smaller fractions (7.3% and 5.2%, respectively). These results indicate that the principal robustness bottleneck of current models arises from generating executable code, rather than from downstream structural checks.

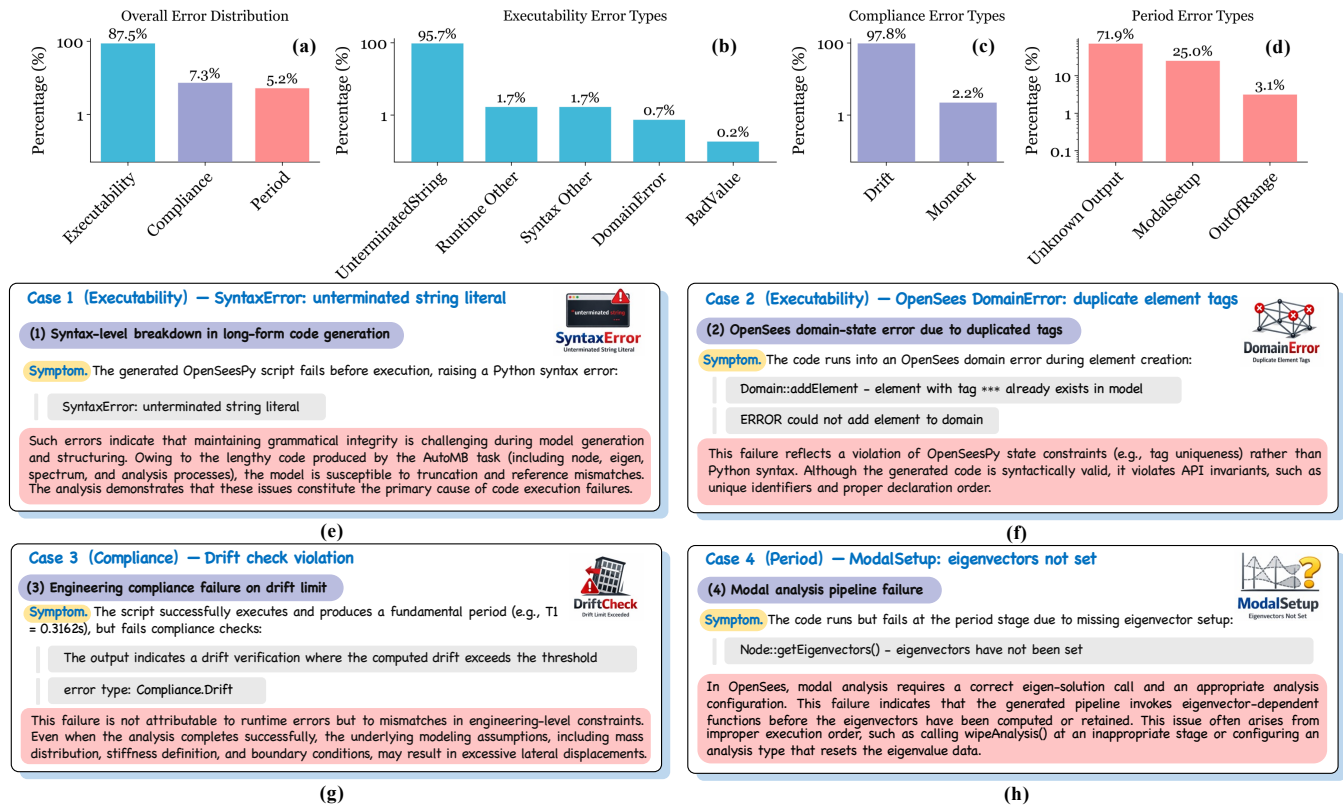


Figure 6: The Limitations of AI-Generated AutoBM Task. An analysis based on 640 sets of modeling code generated by Gemini-2.5-Flash. Subfigures (a–d) present the distribution of error categories, (e–h) provide detailed analyses of individual cases.

Stage-wise error concentration. At each failure stage, errors were not broadly distributed but were instead concentrated in a small number of dominant modes. Specifically:

Executability (Figure 6(b)): `SyntaxError: unterminated string literal` accounted for 95.7% of executability failures. This finding suggests that preserving syntactic integrity remains a major challenge for AutoBM when generating long scripts, particularly those with extensive node definitions and multi-step analysis pipelines.

Compliance (Figure 6(c)): `Compliance.Drift` was the predominant failure mode. This outcome implies that even when execution succeeds and modal results are produced, the synthesized structural models frequently violate engineering constraints due to excessive or unacceptable lateral drift.

Period (Figure 6(d)): Failures were primarily attributed to `period`. `Unknown`, followed by `ModalSetup` errors. These patterns indicate persistent difficulty in reliably extracting and validating modal periods, as well as in maintaining correct eigen-solution configurations required by the analysis workflow.

Figures 6(e–h) present four representative failure cases. Specifically, these failures span multiple layers, ranging from syntactic integrity to simulator state constraints to engineering compliance. Overall, the strong dominance of a small set of failure modes provides a clear basis for developing targeted mitigation strategies.

7 Conclusion

This paper investigates the capability limits of LLMs on the AutoBM task. To address the deficiencies of general-purpose models, a domain-specific dataset, CivilInstruct, and a two-stage fine-tuning strategy guided by structural and physical constraints are proposed. In addition, a physics-aware evaluation benchmark, BMEval, is developed to provide engineering-relevant performance assessment. Results show that supervised instruction fine-tuning significantly improves baseline modeling ability and code executability. Building on this, physically constrained reinforcement learning further enhances physical consistency and specification compliance. Ablation studies confirm the complementary roles of the two stages, with SFT enabling fundamental modeling competence and reinforcement learning reducing physics illusion. Overall, the findings demonstrate that reliable AutoBM performance requires domain-specific data, physics-guided model alignment, and physics-aware evaluation, rather than generic reasoning alone.

8 Acknowledgments

The authors gratefully acknowledge the support from the National Natural Science Foundation of China (Grant Nos. U24A20177 and 52408553) and the International Collaboration Program of Sichuan Province (Grant No. 2025YFHZ0132).

References

- [1] Josh Achiam, Steven Adler, Sandhini Agarwal, Lama Ahmad, Ilge Akkaya, Florencia Leoni Aleman, Diogo Almeida, Janko Altenschmidt, Sam Altman, and Shyamal Anadkat. 2023. *Gpt-4 technical report*. arXiv:2303.08774 doi:10.48550/arXiv.2303.08774
- [2] Aaron Adcock, Aayushi Srivastava, Abhimanyu Dubey, Abhinav Jauhri, Abhinav Pande, Abhinav Pandey, Abhinav Sharma, Abhishek Kadian, Abhishek Kumawat, and Adam Kelsey. 2026. *The Llama 4 Herd: Architecture, Training, Evaluation, and Deployment Notes*. arXiv:2601.11659
- [3] Carlos Avila, Daniel Ilbay, Paola Tapia, and David Rivera. 2025. Toward Responsible AI in High-Stakes Domains: A Dataset for Building Static Analysis with LLMs in Structural Engineering. *Data* 10, 11 (2025), 169. doi:10.3390/data10110169
- [4] Mehmet Baris Batukan and Oya Mercan. 2024. ModularBuildingPy: A Python-Based Numerical Modeling and Analysis Tool for Volumetric Modular Steel Buildings. In *Canadian Society of Civil Engineering Annual Conference*. Springer, 309–320. doi:10.1007/978-3-032-01078-0_26
- [5] Arihant Bedagkar, Sayandeeb Mitra, Raveendra Medicherla, Ravindra Naik, and Samiran Pal. 2025. LLM Driven Smart Assistant for Data Mapping. In *2025 IEEE/ACM 47th International Conference on Software Engineering: Software Engineering in Practice (ICSE-SEIP)*. IEEE, 181–191. doi:10.1109/ICSE-SEIP66354.2025.00022
- [6] Arihant Bedagkar, Sayandeeb Mitra, Raveendra Medicherla, Ravindra Naik, and Samiran Pal. 2025. *LLM-Driven Stationarity-Aware Expert Demonstrations for Multi-Agent Reinforcement Learning in Mobile Systems*. arXiv:2511.19368 doi:10.48550/arXiv.2511.19368
- [7] Patrick Beutler, Manuel Biedermann, Urs Hofmann, Ralph Rosenbauer, and Mirko Meboldt. 2022. Automated Design Workflow for Structural Nodes of Space Frame Structures. *Procedia CIRP* 109 (2022), 419–424. doi:10.1016/j.procir.2022.05.272
- [8] Nicolas Bougie and Narimawa Watanabe. 2025. Citysim: Modeling urban behaviors and city dynamics with large-scale llm-driven agent simulation. In *Proceedings of the 2025 Conference on Empirical Methods in Natural Language Processing: Industry Track*. 215–229. doi:10.18653/v1/2025.emnlp-industry.15
- [9] Huaben Chen, Wenkang Ji, Lufeng Xu, and Shiyu Zhao. 2023. *Multi-agent consensus seeking via large language models*. arXiv:2310.20151 doi:10.48550/arXiv.2310.20151
- [10] Gheorghe Comanici, Eric Bieber, Mike Schaeckermann, Ice Pasupat, Noveen Sachdeva, Inderjit Dhillon, Marcel Blstein, Ori Ram, Dan Zhang, and Evan Rosen. 2025. *Gemini 2.5: Pushing the frontier with advanced reasoning, multimodality, long context, and next generation agentic capabilities*. arXiv:2507.06261 doi:10.48550/arXiv.2507.06261
- [11] Ahmet Bahaddin Ersöz, Onur Pekcan, and Emre Akbas. 2024. AIDCON: An Aerial Image Dataset and Benchmark for Construction Machinery. *Remote Sensing* 16, 17 (2024), 3295. doi:10.3390/rs16173295
- [12] Ziheng Geng, Jiachen Liu, Ran Cao, Lu Cheng, Haifeng Wang, and Minghui Cheng. 2025. *A lightweight large language model-based multi-agent system for 2d frame structural analysis*. arXiv:2510.05414 doi:10.48550/arXiv.2510.05414
- [13] Vinícius Pereira Gonçalves, Andre Luiz Marques Serrano, Gabriel Arquelau Pimenta Rodrigues, Matheus Noschang de Oliveira, Rodolfo Ipolito Meneguette, Guilherme Dantas Bispo, Maria Gabriela Mendonça Peixoto, and Geraldo Pereira Rocha Filho. 2025. An Empirically Validated Framework for Automated and Personalized Residential Energy-Management Integrating Large Language Models and the Internet of Energy. *Energies* 18, 14 (2025), 3744. doi:10.3390/en18143744
- [14] Xingquan Guan, Henry Burton, and Thomas Sabol. 2020. Python-based computational platform to automate seismic design, nonlinear structural model construction and analysis of steel moment resisting frames. *Engineering Structures* 224 (2020), 111199. doi:10.1016/j.engstruct.2020.111199
- [15] Daya Guo, Qiaohu Zhu, Dejian Yang, Zhenda Xie, Kai Dong, Wentao Zhang, Guanting Chen, Xiao Bi, Yu Wu, and YK Li. 2024. *DeepSeek-Coder: When the Large Language Model Meets Programming—The Rise of Code Intelligence*. arXiv:2401.14196 doi:10.48550/arXiv.2401.14196
- [16] Pengwei Guo, Weinan Meng, and Yi Bao. 2024. Knowledge graph-guided data-driven design of ultra-high-performance concrete (UHPC) with interpretability and physicochemical reaction discovery capability. *Construction and Building Materials* 430 (2024), 136502. doi:10.1016/j.conbuildmat.2024.136502
- [17] Mahdi Heshmati, Alireza Khatami, and Hamzeh Shakib. 2021. FEMA P695 methodology for safety margin evaluation of steel moment resisting frames subjected to near-field and far-field records. *SN Applied Sciences* 3, 2 (2021), 185. doi:10.1007/s42452-021-04230-2
- [18] Siming Huang, Tianhao Cheng, Jason Klein Liu, Weidi Xu, Jiaran Hao, Liuyihan Song, Yang Xu, Jian Yang, Jiabing Liu, Chenchen Zhang, et al. 2025. Opencoder: The open cookbook for top-tier code large language models. In *Proceedings of the 63rd Annual Meeting of the Association for Computational Linguistics (Volume 1: Long Papers)*. 33167–33193. doi:10.18653/v1/2025.acl-long.1591
- [19] Jaewon Jeoung, Seunghoon Jung, and Taehoon Hong. 2025. Zero-shot framework for construction equipment task monitoring. *Computer-Aided Civil and Infrastructure Engineering* (2025). doi:10.1111/mice.13506DigitalObjectIdentifier(DOI)
- [20] Yongqing Jiang, Jianze Wang, Xinyi Shen, and Kaoshan Dai. 2025. Large language model for post-earthquake structural damage assessment of buildings. *Computer-Aided Civil and Infrastructure Engineering* 40, 31 (2025), 6324–6342. doi:10.1111/mice.70010DigitalObjectIdentifier(DOI)
- [21] Yongqing Jiang, Jianze Wang, Xinyi Shen, Kaoshan Dai, and Qingzi Ge. 2026. Multitask unified large vision-language model for post-earthquake structural damage assessment of buildings. *Automation in Construction* 182 (2026), 106720. doi:10.1016/j.autcon.2025.106720
- [22] Taegu Kim, Tae Sup Yun, and Hyoung Suk Suh. 2025. Can ChatGPT implement finite element models for geotechnical engineering applications? *International Journal for Numerical and Analytical Methods in Geomechanics* 49, 6 (2025), 1747–1766. doi:10.1002/nag.3956
- [23] Maximilian Kretzschmar, Alexander Gundermann, Jan Mehlstäubl, Alejandro Pradas Gómez, Bernhard Saske, and Kristin Paetzold-Byhain. 2025. Using Role-Specialized LLM Agents for Workflow Execution in a Product Development Setting. In *2025 9th International Conference on Inventive Systems and Control (ICISC)*. IEEE, 642–650. doi:10.1109/ICISC65841.2025.11188152
- [24] Hao Li, Rongzheng Yang, Shuangshuang Xu, Yao Xiao, and Hongyu Zhao. 2024. Intelligent checking method for construction schemes via fusion of knowledge graph and large language models. *Buildings* 14, 8 (2024), 2502. doi:10.3390/buildings14082502
- [25] Yinseng Li, Zhen Dong, and Yi Shao. 2025. *Drafterbench: Benchmarking large language models for tasks automation in civil engineering*. arXiv:2507.11527 doi:10.48550/arXiv.2507.11527
- [26] Haoran Liang, Mohammad Talebi Kalaleh, and Qipei Mei. 2025. *Integrating Large Language Models for Automated Structural Analysis*. arXiv:2504.09754 doi:10.48550/arXiv.2504.09754
- [27] Haoran Liang, Yufa Zhou, Mohammad Talebi Kalaleh, and Qipei Mei. 2025. *Automating Structural Engineering Workflows with Large Language Model Agents*. arXiv:2510.11004 doi:10.48550/arXiv.2510.11004
- [28] DG Lignos, F Zareian, and H Krawinkler. 2010. A steel component database for deterioration modeling of steel beams with RBS under cyclic loading. In *Structures Congress 2010*. 1241–1252. doi:10.1061/41130(369)113
- [29] Haoran Luo, Yikai Guo, Qika Lin, Xiaobao Wu, Xinyu Mu, Wenhao Liu, Meina Song, Yifan Zhu, Luu Anh Tuan, et al. 2025. *Kbqa-ol: Agentic knowledge base question answering with monte carlo tree search*. arXiv:2501.18922 doi:10.48550/arXiv.2501.18922
- [30] Renqian Luo, Lai Sun, Yingce Xia, Tao Qin, Sheng Zhang, Hoifung Poon, and Tie-Yan Liu. 2022. BioGPT: generative pre-trained transformer for biomedical text generation and mining. *Briefings in bioinformatics* 23, 6 (2022), bbac409. doi:10.1093/bib/bbac409
- [31] Iolanda Nuzzo, Francesca Ciliento, and Nicola Caterino. 2020. DIBRAST: a computer-aided seismic design procedure for frame structures equipped with hysteretic devices. *Frontiers in Built Environment* 6 (2020), 13. doi:10.3389/fbuil.2020.00013
- [32] Sandeep Pandey, Ran Xu, Wenkang Wang, and Xu Chu. 2025. OpenFOAMGPT: A retrieval-augmented large language model (LLM) agent for OpenFOAM-based computational fluid dynamics. *Physics of Fluids* 37, 3 (2025). doi:10.1063/5.0257555
- [33] Sizhong Qin, Hong Guan, Wenjie Liao, Yi Gu, Zhe Zheng, Hongjing Xue, and Xinzheng Lu. 2024. Intelligent design and optimization system for shear wall structures based on large language models and generative artificial intelligence. *Journal of Building Engineering* 95 (2024), 10996. doi:10.1016/j.jobe.2024.10996
- [34] Md Nishat Raihan, Antonios Anastasopoulos, and Marcos Zampieri. 2025. mHumanEval-a multilingual benchmark to evaluate large language models for code generation. In *Proceedings of the 2025 Conference of the Nations of the Americas Chapter of the Association for Computational Linguistics: Human Language Technologies (Volume 1: Long Papers)*. 11432–11461. doi:10.18653/v1/2025.nacl-long.570
- [35] Shima Sdeghzadeh, Cristoforo Demartino, and Camillo Nuti. 2025. Modeling of the Colle Castino Bridge in OpenSeesPy for Structural and Seismic Analysis. *Proceedings of the 2024 Eurasian OpenSees Days* 638 (2025), 97. doi:10.1007/978-3-031-90690-9_9
- [36] ByteDance Seed, Yuyu Zhang, Jing Su, Yifan Sun, Chenguang Xi, Xia Xiao, Shen Zheng, Anxiang Zhang, Kaibo Liu, and Daoguang Zan. 2025. *Seed-coder: Let the code model curate data for itself*. arXiv:2506.03524 doi:10.48550/arXiv.2506.03524
- [37] Karan Singhal, Tao Tu, Juraj Gottweis, Rory Sayres, Ellery Wulczyn, Mohamed Amin, Le Hou, Kevin Clark, Stephen R Pfohl, Heather Cole-Lewis, et al. 2025. Toward expert-level medical question answering with large language models. *Nature Medicine* 31, 3 (2025), 943–950. doi:10.1038/s41591-024-03423-7
- [38] Ashish Vaswani, Noam Shazeer, Niki Parmar, Jakob Uszkoreit, Llion Jones, Aidan N Gomez, Łukasz Kaiser, and Illia Polosukhin. 2017. Attention is All you Need. In *Advances in Neural Information Processing Systems*, I. Guyon, U. Von Luxburg, S. Bengio, H. Wallach, R. Fergus, S. Vishwanathan, and R. Garnett (Eds.), Vol. 30. Curran Associates, Inc.
- [39] Qixin Wan, Zilong Wang, Jingwen Zhou, Wanting Wang, Ziheng Geng, Jiachen Liu, Ran Cao, Minghui Cheng, and Lu Cheng. 2025. *Som-1k: A thousand-problem benchmark dataset for strength of materials*. arXiv:2509.21079 doi:10.48550/arXiv.2509.21079

[40] Jason Wei, Xuezhi Wang, Dale Schuurmans, Maarten Bosma, brian ichter, Fei Xia, Ed Chi, Quoc V Le, and Denny Zhou. 2022. Chain-of-thought prompting elicits reasoning in large language models. In *Advances in Neural Information Processing Systems*, S. Koyejo, S. Mohamed, A. Agarwal, D. Belgrave, K. Cho, and A. Oh (Eds.), Vol. 35. Curran Associates, Inc., 24824–24837.

[41] Shijie Wu, Ozan Irsoy, Steven Lu, Vadim Dabrowski, Mark Dredze, Sebastian Gehrmann, Prabhanjan Kambadur, David Rosenberg, and Gideon Mann. 2023. Bloomberggpt: A large language model for finance. arXiv:2303.17564 doi:10.48550/arXiv.2303.17564

[42] Can Xu, Qingfeng Sun, Kai Zheng, Xiubo Geng, Pu Zhao, Jiazhan Feng, Chongyang Tao, Qingwei Lin, and Daxin Jiang. 2024. WizardLM: Empowering large pre-trained language models to follow complex instructions. arXiv:2304.12244 doi:10.48550/arXiv.2304.12244

[43] Xiaorui Xue, Jiansong Zhang, and Yunfeng Chen. 2024. Question-answering framework for building codes using fine-tuned and distilled pre-trained transformer models. *Automation in Construction* 168 (2024), 105730. doi:10.1016/j.autcon.2024.105730

[44] Yexiang Yan and Yazhou Xie. 2025. opstool: A Python library for OpenSeesPy analysis automation, streamlined pre-and post-processing, and enhanced data visualization. *SoftwareX* 30 (2025), 102126. doi:10.1016/j.softx.2025.102126

[45] An Yang, Anfeng Li, Baosong Yang, Beichen Zhang, Binyuan Hui, Bo Zheng, Bowen Yu, Chang Gao, Chengan Huang, and Chenxu Lv. 2025. Qwen3 technical report. arXiv:2505.09388 doi:10.48550/arXiv.2505.09388

[46] Fan Yang and Jiansong Zhang. 2024. Prompt-based automation of building code information transformation for compliance checking. *Automation in Construction* 168 (2024), 105817. doi:10.1016/j.autcon.2024.105817

[47] Rui Ye, Shuo Tang, Rui Ge, Yaxin Du, Zhenfei Yin, Siheng Chen, and Jing Shao. 2025. MAS-GPT: Training LLMs to build LLM-based multi-agent systems. arXiv:2503.03686 doi:10.48550/arXiv.2503.03686

[48] Zhaojian Yu, Yilun Zhao, Arman Cohan, and Xiao-Ping Zhang. 2025. HumanEval pro and MBPP pro: Evaluating large language models on self-invoking code generation task. In *Findings of the Association for Computational Linguistics: ACL 2025*, 13253–13279. doi:10.18653/v1/2025.findings-acl.686

[49] F Zareian, DG Lignos, and H Krawinkler. 2010. Evaluation of seismic collapse performance of steel special moment resisting frames using FEMA P695 (ATC-63) methodology. In *Structures Congress 2010*, 1275–1286. doi:10.1061/(369)116

[50] Wuyang Zhang, Yansong Li, Zeyu Dong, Yu Wu, Yingyao Zhou, Duolei Wang, Songsiyu Xing, Chichun Zhou, and Da Shen. 2024. Renaissance of Literate Programming in the Era of LLMs: Enhancing LLM-Based Code Generation in Large-Scale Projects. arXiv:2502.17441 doi:10.48550/arXiv.2502.17441

[51] Zhu Zhongming, Lu Linong, Yao Xiaona, Zhang Wangqiang, and Liu Wei. 2009. Ministry of housing and urban-rural development of the people's republic of china. (2009).

[52] Ting Zhou, Kezhao Sun, Zhihua Chen, Zhixi Yang, and Hongbo Liu. 2023. Automated optimum design of light steel frame structures in Chinese Rural areas using building information modeling and simulated annealing algorithm. *Sustainability* 15, 11 (2023), 9000. doi:10.3390/su15119000

[53] Minjie Zhu, Frank McKenna, and Michael H Scott. 2018. OpenSeesPy: Python library for the OpenSees finite element framework. *SoftwareX* 7 (2018), 6–11. doi:10.1016/j.softx.2017.10.009

Appendix

A BMBench Implementation Details

A.1 CivilInstruct Dataset Construction Details

Part 1: Fine-Grained Supervised Data. A supervised dataset comprising 3,881 instruction-code pairs was constructed through the systematic parsing of official OpenSeesPy documentation in conjunction with LLM synthesis. Designed to facilitate instruction adherence and automated structural modeling, each data instance comprises two core components: task-oriented natural language instructions derived from standard usage protocols and executable code templates adhering to strict documentation specifications. To enhance model interpretability and eliminate ambiguity during the learning process, detailed line-by-line annotations were incorporated into the code. These annotations provide engineering-level semantic interpretations of key variables and parameters. Comprehensive coverage of core functional modules is provided, encompassing structural modeling, numerical analysis, reliability analysis, and pre- and post-processing. In contrast to general-purpose codebases,

which frequently lack domain semantics or exhibit non-standard API usage, CivilInstruct rigorously ensures the clarity of variable semantics and the consistency of documentation specifications.

Table 3: Engineering Parameter Ranges for Random Structural Sample Generation

Parameter	Value Range / Set
Building Function	{Office, Residential, Mall, Hospital, School, Factory}
Number of Stories	Integer $\in [3, 7]$
Story Height	Uniform $\sim [3.0, 4.0]$ m
Total Height	$H < 23.0$ m
Plan Dimensions	Uniform $\sim [40, 100]$ m, subject to $W \leq L$
Seismic Intensity	{7, 7.5, 8, 8.5, 9}
Peak Ground Acceleration	{0.10, 0.15, 0.20, 0.30, 0.40} g
Seismic Group	{1, 2, 3}
Site Class	{I ₀ , I ₁ , II, III, IV}

Part 2: Parameterized Generated Long Code Data. Approximately 3,100 structural instances were constructed via the stochastic sampling of key architectural and seismic parameters within predefined valid engineering domains. These sampling parameters include building function, story count, and story heights (see Table 3 for complete parameter ranges and discrete value sets). While the selected parameter domains align with prevalent seismic design practices and national codes (e.g., JGJ/T 415-2017 [51]), excessively rigid code-specific constraints were avoided to ensure the generalizability of data-driven learning. For each instance, the LLM first synthesized structural design solutions that conform to engineering principles. Subsequently, building attributes and design solutions were integrated into a specific instruction template (see Appendix A), which guided the model in generating complete, task-specific code. To enhance the diversity of instruction distributions, 1,000 instruction variants were derived from the original template, adopting the approach of Xu et al. [42]. The resulting programs typically comprise approximately 600 lines of executable code, encompassing the entire workflow from structural modeling to analysis and validation. To ensure rigorous data quality control, automated validation of all generated code was performed, with quantitative scores assigned based on code quality and task completion. Ultimately, only high-quality samples were retained for the second stage of reinforcement learning training. At the same time, data about execution failures were segregated for use in constructing the Part 3 data component.

Part 3: Execution Error-Oriented Debugging of CoT Data. A specialized Bug-CoT dataset was constructed through the systematic analysis of execution failures identified in Part 2. Detailed debugging information was captured for these failure samples, encompassing error logs, return codes, runtime environments, and contextual metadata. A distinguishing characteristic of this dataset is its bug-driven generation mechanism. Unlike synthetic defects, these errors arise from complex, coupled interactions between the

OpenSeesPy API, the numerical solver, and the modelling logic. Consequently, they are representative of authentic challenges encountered in actual engineering analyses. For each documented error, the LLM was employed to generate a structured debugging CoT, comprising a problem description, root cause analysis, resolution strategy, and prevention guidelines. Furthermore, to enhance data coverage and inference robustness, each original error was expanded into multiple semantically related yet distinct variants. Ultimately, all inference pathways were converted into a question-and-answer format, providing fine-grained supervisory signals to train the model in the systematic debugging of extended scientific computing sequences.

Part 4: Physics-Informed Expert Data. Based on the extensive codebases generated in Part 2, a high-quality expert dataset was curated for the subsequent reinforcement learning stage. Specifically, through the implementation of automated execution and multidimensional quantitative scoring, which encompasses code executability and compliance with design specifications, 512 sample sets achieving scores exceeding 90 out of 100 were isolated from the pool of executable code. These samples not only demonstrate runtime robustness but also adhere to stringent engineering constraints. To provide robust and physically interpretable training signals for reinforcement learning, the structural fundamental period, a critical metric in dynamics, was extracted to serve as the ground truth. As a pivotal parameter in seismic design, this indicator possesses distinct physical significance. Consequently, it serves as an effective supervisory signal, guiding the model toward acquiring a structural logic that aligns with engineering rationality.

A.2 BMEval Construction Details

Structural Cycle Consistency Assessment ($\text{Pass}@k_{\text{period}}$). Because program executability alone is insufficient to satisfy stringent engineering requirements, the numerical rationality of the generated outputs was further evaluated. This study focuses on the first-order natural vibration period of the structure, denoted as T_1 , and extracts the predicted values from program outputs using a deterministic, rule-based matching method. If the relative error between the predicted value and the ground-truth value satisfies the following criterion:

$$\frac{|T_1^{\text{Pred}} - T_1^{\text{gt}}|}{T_{\text{gt}}} \leq \epsilon \quad (16)$$

Here, T_{gt} denotes the reference ground-truth, and the allowable relative error threshold adopted in this experiment is set to 0.30. The resulting $\text{Pass}@k_{\text{period}}$ metric, calculated according to this criterion, is intended to quantify the model's engineering-level numerical accuracy.

Engineering Compliance Assessment ($\text{Pass}@k_{\text{compliance}}$). In addition to numerical accuracy, engineering analysis results must provide explicit conclusions regarding compliance with specifications or safety verification. To address this requirement, engineering compliance evaluation indicators were introduced to assess whether the program output clearly articulates a conclusion that satisfies design verification criteria. Methodologically, a conservative keyword-matching strategy was adopted, in which affirmative

terms (e.g., “pass”, “satisfy”) were identified, while negative semantic processing mechanisms were incorporated to reduce the risk of misclassification. If a program, following successful execution, produces a verification conclusion that conforms to the relevant engineering specifications, it is considered to have passed the compliance assessment.

Joint Evaluation Indicator ($\text{Pass}@k_{\text{strict}}$). To comprehensively assess the AutoBM capabilities of the model under realistic engineering application scenarios, a more stringent composite evaluation criterion was defined. A generated code sample is considered strictly correct only if it simultaneously satisfies the following three necessary conditions: (1) the program executes successfully without exceptions; (2) the extracted structural period prediction falls within the prescribed allowable error range; and (3) the output includes an explicit conclusion confirming compliance with relevant design specifications. The $\text{Pass}@k_{\text{strict}}$ indicator, calculated according to this criterion, represents the most rigorous comprehensive performance metric employed in this study and most effectively reflects the model's practical value in real-world engineering applications.

In Figure 7, the correlation matrix of building attributes is presented, demonstrating the rationality and diversity of the BMEval distribution.

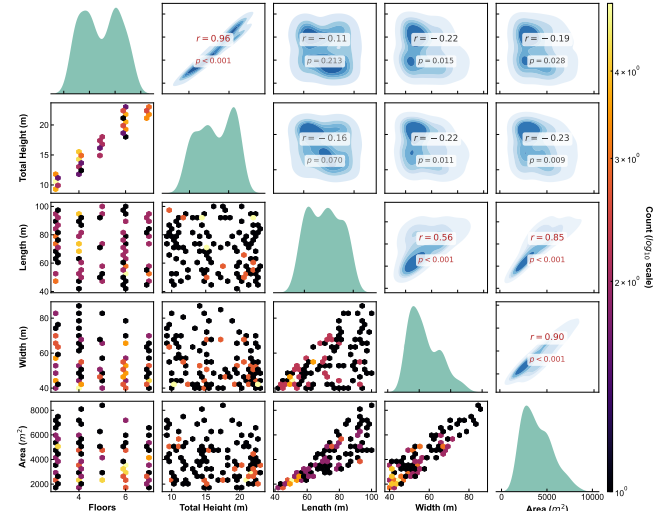


Figure 7: Building Attributes Correlation Matrix

B Prompt used in AutoBM

B.1 Prompt Template for Structural Design and Modeling Code Generation

To generate analysis-ready reinforced concrete (RC) frame models in a consistent and code-compliant manner, we adopt a rule-constrained, prompt-based design workflow (as shown in Figure 8). Domain-specific knowledge from seismic engineering and relevant Chinese design codes (GB50011-2010, GB50010-2010, and JGJ3-2010) is embedded as explicit constraints, requiring the model to output only final, validated structural parameters formatted for direct implementation in OpenSeesPy. The workflow enforces capacity design principles, gravity load limits, seismic detailing requirements,

Structural Design Prompt																																																
Role: You are a structural engineering expert specializing in earthquake engineering, finite element modeling, and reinforced concrete (RC) frame analysis. You are thoroughly familiar with the Chinese codes: Code for Seismic Design of Buildings (GB50011-2010), Code for Design of Concrete Structures (GB50010-2010), and Technical Specification for Concrete Structures of Tall Building (JGJ3-2010). Your task is to complete the design of a reinforced concrete plane frame structure based on the provided building information. The output must be formatted for use in OpenSeesPy modeling. Design response spectrum parameters strictly refer to the information in Tables 1 and 2:																																																
Table 1: Maximum Horizontal Seismic Influence Coefficient (α_{max})			Table 2: Characteristic Period Values $T_g(S)$																																													
<table border="1"> <thead> <tr> <th>Seismic Intensity</th><th>Frequent Earthquake</th><th>Rare Earthquake</th></tr> </thead> <tbody> <tr> <td>Intensity 6</td><td>0.04</td><td>0.28</td></tr> <tr> <td>Intensity 7</td><td>0.08 (0.12)</td><td>0.50 (0.72)</td></tr> <tr> <td>Intensity 8</td><td>0.16 (0.24)</td><td>0.90 (1.20)</td></tr> <tr> <td>Intensity 9</td><td>0.32</td><td>1.40</td></tr> </tbody> </table>			Seismic Intensity	Frequent Earthquake	Rare Earthquake	Intensity 6	0.04	0.28	Intensity 7	0.08 (0.12)	0.50 (0.72)	Intensity 8	0.16 (0.24)	0.90 (1.20)	Intensity 9	0.32	1.40	<table border="1"> <thead> <tr> <th rowspan="2">Design Earthquake Group</th><th colspan="4">Site Class</th></tr> <tr> <th>I₀</th><th>I₁</th><th>II</th><th>III</th><th>IV</th></tr> </thead> <tbody> <tr> <td>Group 1</td><td>0.20</td><td>0.25</td><td>0.35</td><td>0.45</td><td>0.65</td></tr> <tr> <td>Group 2</td><td>0.25</td><td>0.30</td><td>0.40</td><td>0.55</td><td>0.75</td></tr> <tr> <td>Group 3</td><td>0.30</td><td>0.35</td><td>0.45</td><td>0.65</td><td>0.90</td></tr> </tbody> </table>			Design Earthquake Group	Site Class				I ₀	I ₁	II	III	IV	Group 1	0.20	0.25	0.35	0.45	0.65	Group 2	0.25	0.30	0.40	0.55	0.75	Group 3	0.30	0.35	0.45	0.65	0.90
Seismic Intensity	Frequent Earthquake	Rare Earthquake																																														
Intensity 6	0.04	0.28																																														
Intensity 7	0.08 (0.12)	0.50 (0.72)																																														
Intensity 8	0.16 (0.24)	0.90 (1.20)																																														
Intensity 9	0.32	1.40																																														
Design Earthquake Group	Site Class																																															
	I ₀	I ₁	II	III	IV																																											
Group 1	0.20	0.25	0.35	0.45	0.65																																											
Group 2	0.25	0.30	0.40	0.55	0.75																																											
Group 3	0.30	0.35	0.45	0.65	0.90																																											
Building Information <i>Random generated by the program</i>																																																
Output Requirements Strictly adhere to the following structured format to output the design parameters in English, suitable for subsequent OpenSeesPy modeling. The output must be limited to key information only. Do not provide any calculation processes, reasoning, design summaries, or additional explanations. All parameters must be reasonably derived based on codes and engineering experience to ensure accuracy and consistency. Beam and column section design results must be listed separately by floor. The entire design scheme must strictly ensure that beam and column members satisfy capacity requirements under the ultimate design load combinations of dead and live loads, and detailing must strictly meet code requirements (e.g., minimum reinforcement ratios, strong-column/weak-beam, strong-shear/weak-bending, etc.). Additionally, ensure that the representative gravity load value in the load takedown remains between 6 kN/m ² and 10 kN/m ² . The design must strictly guarantee convergence of the structural gravity analysis and ensure that displacement checks and component capacity checks satisfy limit values. All values must be final optimized results, ensuring that capacity, stiffness, and displacement limits under load combinations fully comply with the codes:																																																
The final output is organized strictly in accordance with the following templates (I) - (VI):																																																
(I) Grid Scheme <ul style="list-style-type: none"> Spans per bay (X/Y direction separately, Unit: m): Story heights (Unit: m): 			(IV) Beam Design per Floor <ul style="list-style-type: none"> Section Dimensions ($b \times h$, mm): End Section Longitudinal Reinf (Count, Diameter, Location): 																																													
(II) Load Take - down <ul style="list-style-type: none"> Dead/Live Load per m^2: Representative Gravity Load per story, Total Structural Gravity Load: For the selected Plane Frame: Representative Gravity Load per story; Total Frame Gravity Load: Nodal Mass Distribution (Mass at each column top node per floor): Distributed Gravity Load on Beams per floor: 			(V) Column Design per Floor <ul style="list-style-type: none"> Section Dimensions ($b \times h$, mm): End Section Longitudinal Reinf (Count, Diameter, Location): 																																													
(III) Load Combinations <ul style="list-style-type: none"> Combinations used (Dead, Live, Seismic): Note on calculation of design forces: 			(VI) Response Spectrum Params <ul style="list-style-type: none"> α_{max}, T_g, ζ, exc. 																																													
Special Emphases: <ul style="list-style-type: none"> (1) Optimization & Verification Loop: During the verification process, if the design fails to meet any capacity or displacement requirements, you must automatically increase section dimensions and reinforcement ratios. You must iteratively recalculate and adjust the design until the scheme fully satisfies both the inter-story drift limit and all component capacity checks. All output parameters must be the final, optimized values that have been verified to strictly comply with the codes. (2) Exclusive Output Constraint: You are required to output only the final, optimized, and verified design scheme, strictly organized according to the requested structure (specifically containing the complete items I through VI). Do not output any other content, internal reasoning, or intermediate steps. (3) Completeness Mandate: Failure to output the complete set of items (I) through (VI) will be considered a severe error and implies the generation must be restarted. 																																																

Figure 8: Prompt template for structural scheme design

and interstory drift constraints. An implicit verification loop is incorporated, whereby component dimensions and reinforcement configurations are iteratively adjusted until all strength and displacement criteria are satisfied. This framework enables scalable, reproducible integration of LLMs with physics-based structural analysis. As shown in Figure 9, a rule-constrained OpenSeesPy code-generation prompt is employed to deterministically translate the outputs of the Structural Design Prompt into an executable 2D RC frame model. The prompt enforces standardized modeling assumptions, ensures mass consistency with representative gravity loads, and defines a complete analysis pipeline that includes gravity, modal, and response-spectrum analyses, with interstory drift verification. Component forces are automatically evaluated against design capacities to compute demand-to-capacity ratios, thereby establishing a reproducible design, analysis, and verification loop.

B.2 Prompt Template for OpenSeesPy Documentation-Based Dataset Generation

A document-driven data-generation instruction is designed to construct high-quality instruction–code pairs from the official OpenSeesPy

documentation. As shown in Figure 10, strict alignment with documented APIs, mathematical formulations, and usage notes is enforced, resulting in structured JSON output. Each sample comprises a concise natural-language instruction that describes the intended functionality, expected behavior, and engineering context, paired with a well-documented code snippet that includes line-by-line comments and variable-level technical explanations. Multiple diverse samples are generated for each documentation segment to enhance coverage and robustness.

B.3 Prompt Template for Instruction Rewriting

As shown in Figure 11, an instruction-rewriting prompt is used to systematically transform simple instructions into more complex, yet human-interpretable, forms. The rewriting process increases both the depth and breadth of the original requests while enhancing professional tone and technical precision. To preserve generality, the rewritten instructions intentionally avoid introducing specific modeling details or scenario-dependent constraints. Additional constraints on length and redundancy are imposed to ensure consistency and controlled complexity.

Structural Modeling Programming Prompt

Role: As a structural engineering expert familiar with OpenSeesPy code writing and modeling, you need to complete the code writing task based on the following building information and reinforcement requirements.

Building Information

Generated by Structural Design Prompt

OpenSeesPy Programming Tasks

- (1) **Model Definition.** The structural model is defined as a 2D planar frame ($ndm = 2$, $ndf = 3$) established along the X-axis centerline. Global units are defined in Newtons (N) and meters (m). An n -story frame requires the definition of $n + 1$ node levels, indexed from Level 0 (Base) to Level n (Roof). The element distribution consists of beam elements for each floor and $n \times$ (number of bays + 1) column elements.
- (2) **Node and Element Definition.** Nodes and beam-column elements are defined based on the specific story heights and bay widths of the plane frame. Node and element identifiers (IDs) must be defined continuously to avoid conflicts or gaps. Nodes are numbered sequentially following a “Floor-Axis” order: all nodes on a specific level are defined before proceeding to the next level. For an n -story frame, $n + 1$ levels of nodes are generated (Base foundation + n floors). The number of nodes per level is equal to the number of bays + 1 (e.g., a 7-bay frame requires 8 nodes per level). The total number of nodes is calculated as $(\text{stories} + 1) \times (\text{bays} + 1)$.
- (3) **Geometric Nonlinearity.** Geometric transformations are assigned specifically to element types: Linear transformation is used for beam elements, while P-Delta transformation is applied to column elements. All structural members are modeled using the `elasticBeamColumn` element.
- (4) **Mass Definition.** Nodal masses are lumped at the column-top nodes of each floor. The mass distribution is calculated based on the representative gravity load values. The total system mass must correspond exactly to the sum of the representative gravity loads specified in the structural design.
- (5) **Boundary Conditions.** The base nodes (Level 0) are defined with a fixed connection to the ground (fully constrained).
- (6) **Gravity Analysis.** A linear `TimeSeries` and `LoadPattern` are defined to apply gravity loads to the beam and column members. A static analysis is performed to establish the initial structural state under gravity loads.
- (7) **Response Spectrum Analysis.** The response spectrum is defined using the parameters α_{max} , T_g , γ , η_1 , and η_2 . Modal responses are calculated for each mode and combined using the Square Root of the Sum of the Squares (SRSS) method. Inter-story drifts are computed and verified against the limit of 1/550.
- (8) **Modal Analysis.** The analysis configuration includes defining modal analysis load cases. The first three modes of vibration are calculated. Key outputs include the fundamental period and the total system mass.
- (9) **Load Combinations.** Load combinations are defined according to relevant design codes, considering only gravity loads and horizontal seismic actions.
- (10) **Design Verification**
 - **Displacement Check:**
 - Output the maximum inter-story drift and drift ratio for each load combination and compare them against the allowable limits.
 - Violations (if any) are flagged in the console and output files.
 - **Component Capacity Check:**
 - Internal forces in beams and columns are compared against design capacities (derived from reinforcement calculations):
 - $Moment \leq Design\ Moment\ Capacity$
 - $Axial\ Force \leq Design\ Axial\ Capacity$
 - $Shear\ Force \leq Design\ Shear\ Capacity$
 - Output the safety factor or utilization ratio (Demand/Capacity) for each component.
 - **Result Summary:**
 - Generate a comprehensive summary table listing: Load Case, Component ID, Internal Forces, Capacity, Utilization Ratio, Code Compliance status, and Pass/Fail status for both displacement and capacity checks.
- (11) **Result Output**
 - To minimize code length, explicit code for reading/writing variables to external files is omitted.
 - Key results are printed directly to the Python console.
- (12) **Coding Standards and Quality Assurance**
 - **Variable Naming:** Use descriptive, full-word variable names (e.g., `frequency`, `period`, `force`, `moment`) to ensure clarity; avoid single-character or generic names.
 - **Scope Management:** Use distinct prefixes for variables within different functional modules to prevent naming conflicts.
 - **File Operations:** Use explicit naming for file objects (e.g., `file_obj`, `output_file`).
 - **Error Prevention:** Include checks for variable definitions and type validation.
 - **Code Structure:** Encapsulate distinct functionalities into independent functions and use dictionaries to store computation results.
 - **Quality Check:** Perform post-generation checks for variable name duplication and scope conflicts.
 - **Documentation:** Add comments explaining the purpose and data type of critical variables.
 - **OpenSeesPy API Compliance:** Strictly adhere to official syntax
 - Eigenvalue analysis must use `eigenvalues = ops.eigen(numModes)` (avoid invalid arguments like ‘`values`’).
 - A complete solver sequence (`system`, `numberer`, `constraints`, `integrator`, `algorithm`, `analysis`) must be set before every analysis.
 - For modal analysis: Use `ops.system('BandGeneral')` and `ops.numberer('RCM')`.
 - For static analysis: Ensure all solver components are correctly reinitialized.
- (13) **Output Format.** All code is consolidated into a single `.py` file.

Figure 9: Prompt template for structural modeling programming

B.4 Prompt Template for Bug-Fixing Dataset Generation

As shown in Figure 12, a bug-fix-oriented data-generation prompt is designed for OpenSeesPy modeling and debugging. Each sample is structured as a comprehensive question-and-answer pair that covers problem manifestation, root-cause analysis, solution strategies, and preventive practices. Technically grounded explanations aligned with OpenSeesPy internal mechanics, syntax rules, and common user misconceptions are enforced. The resulting dataset emphasizes executable correctness, debugging interpretability, and long-term error avoidance.

C Supplementary Ablation Studies

C.1 RLA-SPC Can Improve Model Performance on AutoBM Task

This section systematically demonstrates the effectiveness of the proposed two-stage fine-tuning strategy with structural physical constraints for the AutoBM task through a series of ablation experiments. In addition, it provides an in-depth analysis of the differentiated contributions of SFT and reward-based optimization to the development of model capabilities. Three experimental configurations were evaluated across three representative baseline models (CodeLlama-7B-Instruct, Qwen2.5-Coder-7B, and Seed-Coder-8B^R): the original baseline model, a model trained using SFT only (stage 1, incorporating data Parts 1-3), and a physically aligned two-stage

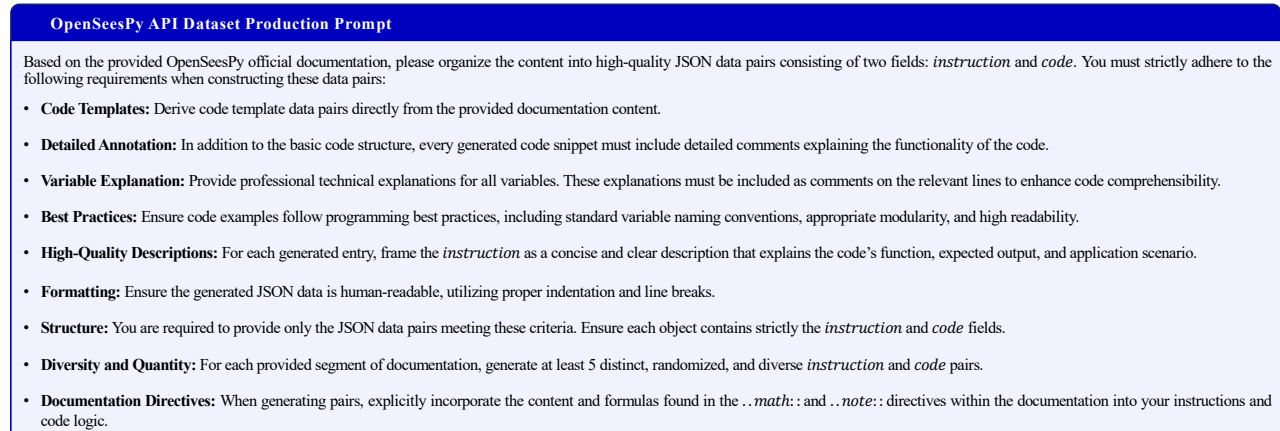


Figure 10: Prompt template for dataset construction based on the OpenSeesPy API

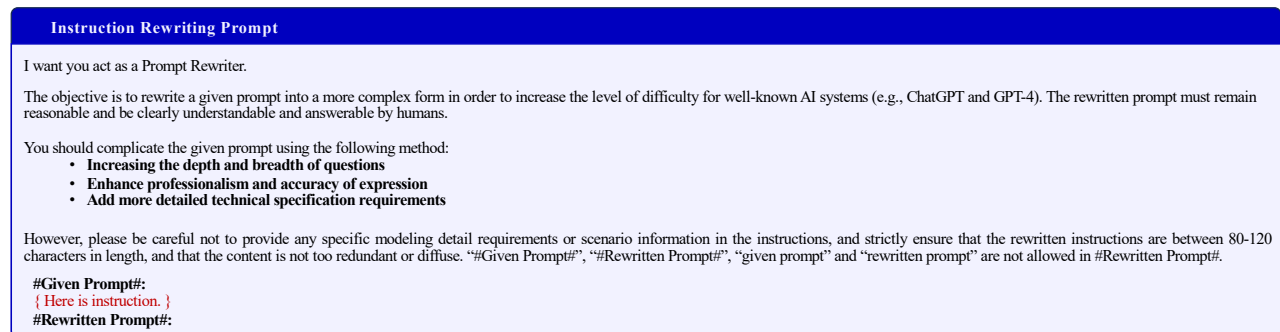


Figure 11: Prompt template for instruction rewriting

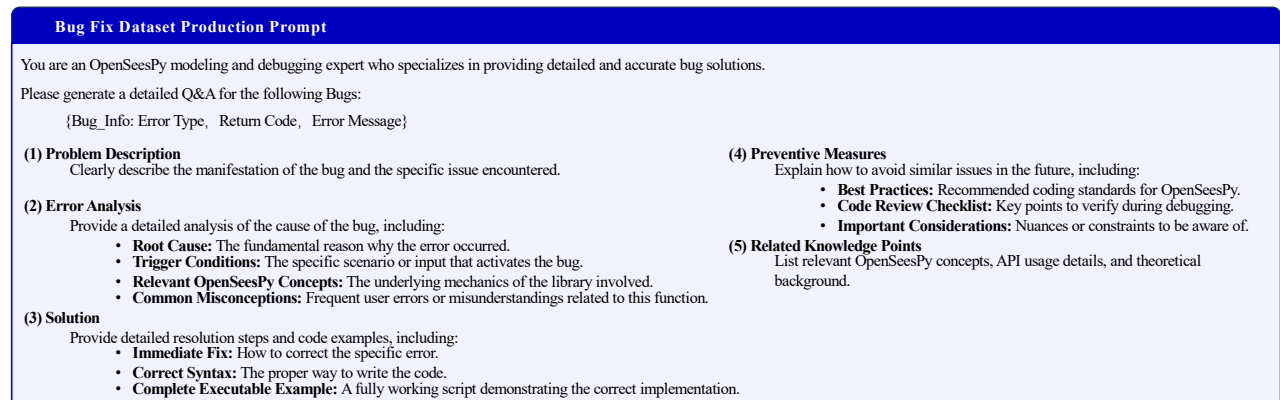


Figure 12: Prompt template for dataset construction based on bug information

model that integrates GRPO (stage 1+2), augmented with data Part 4 and physics-constrained reward signals.

The experimental results (Table 2, Figure 5(b-c)) indicate that SFT plays a decisive role in establishing the model's foundational modeling capability. Compared with the baseline, the code execution rate (Executability) of each model increases substantially

after stage 1 training, demonstrating that the models effectively acquire the syntactic structure and common programming patterns of OpenSeesPy. Although the code generated by SFT-trained models is generally executable, it is often accompanied by "physical illusion" phenomena that violate fundamental mechanical principles or engineering design specifications. With the introduction

of GRPO, the models exhibit stable and significant improvements not only in code executability but also in stringent performance metrics (e.g., $\text{Pass}@5_{strict}$). These results suggest that GRPO effectively enforces physical consistency and specification compliance through explicit reward-based guidance. A comparative analysis further reveals the complementary roles of the two stages: stage 1 establishes basic syntactic executability, whereas stage 2 achieves semantic alignment with physical laws and engineering specifications, thereby substantially reducing the generation of physically implausible outputs.

C.2 Execution Error-Oriented Debugging Chain of Thought Data Ablation Study

This section aims to systematically validate the effectiveness of the CivilInstruct data construction strategy, with particular emphasis on assessing the critical role of the execution-error-driven Bug Fix dataset (Part 3) in enhancing code robustness and engineering reliability. To this end, two SFT data construction schemes were designed for comparison, while maintaining strict consistency in the model architecture and learning strategies. The first scheme uses only Parts 1 and 2 as positive samples for SFT. The second scheme enhances this setup by incorporating Part 3 (Bug-CoT data), allowing the model not only to learn correct coding paradigms during fine-tuning but also to be exposed to real execution failure cases,

along with their systematic error analyses and repair trajectories. Experimental results (Figure 5(d)) demonstrate consistent and substantial performance improvements across all three baseline models (CodeLlama-7B-Instruct, Qwen2.5-Coder-7B, and Seed-Coder-8B^R). Specifically, after introducing the Bug-CoT dataset, the $\text{Pass}@1$ score of CodeLlama-7B-Instruct increased from 50.82% to 55.73%, while its $\text{Pass}@5$ score improved markedly from 56.62% to 67.73%. The Qwen2.5-Coder-7B and Seed-Coder-8B^R models exhibit similar gains, with $\text{Pass}@1$ increases of 4.45% and 2.23%, respectively.

Experimental results indicate that incorporating Part 3 not only enhances code executability but also significantly increases the success rate under stringent engineering constraints. Notably, this improvement does not arise from superficial normalization of output formats, but rather from the model's deeper assimilation of real failure patterns. By learning to recognize low-level syntactic errors, misuse of application programming interfaces, and the underlying causes of structurally unstable configurations, the model can proactively avoid fragile modeling decisions during the generation process, thereby producing more robust candidate solutions. This enriched and higher-quality solution space provides a strong foundation for the subsequent GRPO stage, enabling the reinforcement learning procedure to identify optimal trade-offs between physical constraints and regulatory objectives more efficiently. These effects ultimately manifest as concurrent improvements across multiple key evaluation indicators.